Supporting Information

Aptasensor Based on Fluorophore-quencher Nano-pair and Smartphone Spectrum Reader for On-site Quantification of Multi-pesticides

Nan Cheng[1,2#], Yang Song[2#], Qiangqiang Fu[2], Dan Du[2], Yunbo Luo[1], Yong Wang[3],

Wentao Xu[1] and Yuehe Lin[2*]*

A. Experimental section

3D-printed smartphone-based fluorescence spectrum reader fabrication. The fluorescence apta-LFB spectrometer attachment for iPhone 5 was designed in SolidWorks spectrometer, which mechanically aligns a diffraction grating (GT13-12; Thorlabs Inc., NJ, USA), edgepass filter (NT48-354; Edmund Optics Inc., NJ, USA), and a collimating lens (NT63-491; Edmund Optics Inc.). While holding all components in correct alignment, the system prevents external light sources from reaching the camera. Two commercial compact blue laser diodes (eBay) were used as the excitation light source powered by two AAA batteries to provide narrow-band excitation centered at 405 nm with an output of 5 mW. In order to maximize the collection of singles from the test zone into the camera, the sample was illuminated at an orthogonal angle (60 degree) to the light collection axis. The fluorescence emission was collected and separated from the excitation and background via one edgepass filter positioned behind the sample. The point of the edgepass filter was situated at the same center point of the illuminating zone. The opposing focal point of the collection lens was located at the end face of an optical fiber (core diameter = 1 mm). The fluorescence emission was focused along only one axis onto the transmission diffraction grating (1,200 lines/mm) at a 47 degree angle with respect to the light path in order to satisfy the grating first-order diffraction mode. Magnified fluorescent spectrum images were formed and collected with both the external and the built-in lens of the iPhone camera, then recorded by the CMOS sensor chip. The internal camera is sensitive to wavelengths within the visible spectrum, $400 < \lambda < 700$ nm. Pixel

values read from the smartphone camera were converted to wavelength by using three laser pointers (405, 532, and 650 nm) to calibrate the pixel-wavelength relationship. Three bands were produced in the acquired image when the system was illuminated with the laser pointers. We used the known laser wavelengths determined by a reference spectrometer to assign wavelength values to pixel values along the spectral direction of the camera image. A linear relationship between wavelength value and pixel index results in a single-pixel wavelength increment of 0.253 nm/pixel. The resolution is limited by the camera lenses. For spectrum analysis, a symmetry center line of the spectrum was first determined, then the intensity of each wavelength point was obtained by calculating the sum of the red, green, and blue values.

Laser angle optimization. We used an optical stage to rotate the test strips and optical sensor about two axes. An Ocean optical light source irradiated the test strips and a USB40000 spectrometer measured the light intensity during the rotation. We measured the test zone intensity in SpectraSuit software in real time to reduce temporal variations. As shown in **Figure S9**, any effective increase in the test zone signal on the test strips improved the signal-to-noise (SNR) ratio by minimizing the light scatter from the nitrocellulose membrane. **Figure S10** shows the results from the calibration system, in which each data point demonstrated the intensity of the test zone divided by background signal (mostly scatter light). The signal increased as the scattered light from the test zone decreased. The 60 degree of angle of irradiation light from the detection position showed greatest SNR ratio. If we had continued to increase the irratiation angle, the signal would have increased further but the test zone would have lost the light transmission. Per the same principle, the detection angle from the test zone should have been 90 degrees due to maximal focus of the emission signal from the nitrocellulose membrane.

Characterization. The morphologies of the nanomaterial were characterized by transmission electron microscopy (TEM) on a Philips CM200 UT (Field Emission Instruments, USA) at an accelerating voltage of 40 KV. The zeta potential was measured using a zeta potential analyser (Brookhaven Instruments Co, USA). UV/vis spectroscopy was performed with a QuantaMasterTM40 spectrophotometer under the external excitation of a 250 mW 980 nm laser diode (RGB Laser systems). The fluorescence spectra were measured with a Cary Eclipse fluorimeter. The decay curves were acquired over the entire emission range on Ultima^{TM}

Lifetime Fluorescence Spectrofluorometer (HORIBA Scientific, UK). X ray photoelectron spectral (XPS) analysis was performed with a Surface Science Instrument SSX-100. All measurements were performed at room temperature.

B. Supplementary tables

Table S1. Oligonucleotides used in this study

Oligonucleotide name	Sequence (5'-3')	Reference
CBA	Thio/MC6-D/-CGAATTTCTTCCATTTCTTGCTTCTTGCATGGATTCG	[1]
DBA	Thio/MC6-D/-ATCCGTCACACCTGCTCTAATATAGAGGTATTGCTCTTGGACAAGGTACAG GGATGGTGTTGGCTCCCGTAT	[2]
MBA	Thio/MC6-D/-ATCCGTCACACCTGCTCTTATACACAATTGTTTTTCTCTTAACTTCTTGACTG CTGGTGTTGGCTCCCGTAT	[3]
BCS-C	Biotin/-CGAATCCATGCAAGAAGCAAGAAATGGAAGAAATTCG	/
BCS-D	Biotin/-ATACGGGAGCCAACACCATCCCTGTACCTTGTCCAAGAGCAATACCTCTATATTA GAGCA GGTGTGACGGAT	/
BCS-M	Biotin/-ATACGGGAGCCAACACCAGCAGTCAAGAAGTTAAGAGAAAAACAATTGTGTATA AGAGCA GGTGTGACGGAT	/

References

[1]Y. Jiao, H. Jia, Y. Guo, H. Zhang, Z. Wang, X. Sun, J. Zhao, *RSC Adv.* **2016**, *6*, 58541-58548.

[2]M. Jokar, M. H. Safaralizadeh, F. Hadizadeh, F. Rahmani, M. R. Kalani, *J. Biomol. Struct. Dyn.* **2017**, *35*, 343-353.

[3]R. Bala, M. Kumar, K. Bansal, R. K. Sharma, N. Wangoo, *Biosens.Bioelectron.***2016**, *85*, 445-449.

Table S2. Maximum residue levels of agricultural products across various countries, organizations (available online)

Countries and organizations	Research Websites
Codex Alimentarius	http://www.fao.org/fao-who-codexalimentarius/standards/pestres/pesticides/en/
The European Union	http://ec.europa.eu/food/plant/pesticides/eu-pesticides-database/public/?event=pesticide.residue.selection&language=EN
The United States	https://www.ecfr.gov/cgi-bin/retrieveECFR?gp=1&SID=4451dd069311a99184f2c3a4126293eb&ty=HTML&h=L&mc=true&n=pt40.24.180&r=PART
China	http://202.127.42.84/tbt-sps/mrlsdb/mrlsdb.do
Canada	http://pr-rp.hc-sc.gc.ca/mrl-lrm/index-eng.php
Japan	http://www.m5.ws001.squarestart.ne.jp/foundation/search.html

Table S3. Comparison among previously reported biosensors for pesticide determination

Target	Biosensor	Recognition Element	LOD	Multiple Detection	Reader Type	Reference
Chlorpyrifos	Electrochemical Biosensor	Acetylcholinesterase	0.02 ng/mL	No	Electrochemical workstation	[1]
Chlorpyrifos	Electrochemical Biosensor	Aptamer	0.33 ng/mL	No	Electrochemical workstation	[2]
Chlorpyrifos	Photoelectrochemical Biosensor	Acetylcholinesterase	0.3 ng/mL	No	Electrochemical analyzer	[3]
Chlorpyrifos	Electrochemical Biosensor	Acetylcholinesterase	0.23 μM	No	Electrochemical workstation	[4]
Chlorpyrifos	Colorimetric Biosensor	Antibody	2.5 ng/mL	No	Naked eye for qualitative determination	[5]
Chlorpyrifos	**Fluorescence biosensor**	**Aptamer**	**0.73 ng/mL**	**Yes**	**Smartphone-based Portable Reader**	**This work**
Diazinon	Impedimetric Biosensor	Lipase	10 nM	No	Electrochemical workstation	[6]
Diazinon	Potentiometric biosensor	Acetylcholinesterase	6 -10 μg/mL	No	Electrochemical workstation	[7]
Diazinon	Colorimetric Biosensor	Antibody	1 ng/mL	No	Naked eye for qualitative determination	[8]
Diazinon	Colorimetric Biosensor	Aptamer	17.903 nM	No	UV-Vis absorption spectrum	[9]
Diazinon	**Fluorescence biosensor**	**Aptamer**	**6.7 ng/mL**	**Yes**	**Smartphone-based Portable Reader**	**This work**
Malathion	Colorimetric Biosensor	Acetylcholinesterase	2.5 μg/mL	No	Visual comparison or spectrophotometric measurements	[10]
Malathion	Optical Biosensor	Aptamer	3.3 μg/mL	No	Surface-Enhanced Raman Spectroscopy	[11]

Malathion	Colorimetric Biosensor	Aptamer	1.94 pM	No	UV-Vis absorption spectrum	[12]
Malathion	Colorimetric Biosensor	Aptamer	0.06 pM	No	UV-Vis absorption spectrum	[13]
Malathion	**Fluorescence biosensor**	**Aptamer**	**0.74 ng/mL**	**Yes**	**Smartphone-based Portable Reader**	**This work**

References

1.Wang, H., Zhao, G., Chen, D., Wang, Z., Liu, G., *Int. J. Electrochem. Sci* **2016,** *11*, 10906-10918.
2.Jiao, Y., Jia, H., Guo, Y., Zhang, H., Wang, Z., Sun, X., Zhao, J., *RSC Adv.* **2016,** *6* (63), 58541-58548.
3.Mao, H., Yan, Y., Hao, N., Liu, Q., Qian, J., Chen, S., Wang, K., *Sens. ctuators B Chem.***2017,** *238*, 239-248.
4.Zhang, Y., Xia, Z., Li, Q., Gui, G., Zhao, G., Lin, L., *J.Electrochem Soc.***2017,** *164* (2), B48-B53.
5.Kim, Y. A., Lee, E.-H., Kim, K.-O., Lee, Y. T., Hammock, B. D., Lee, H.-S., *Anal. Chim. Acta* **2011,** *693* (1), 106-113.
6.Zehani, N., Dzyadevych, S. V., Kherrat, R., Jaffrezic-Renault, N. J., *Front.Chem.***2014,** *2*.
7.Ramadhan, L., Jahiding, M. Materials Science and Engineering, IOP Publishing: **2016**, p 012013.
8.Lee, J.-Y., Kim, Y. A., Kim, M. Y., Lee, Y. T., Hammock, B. D., Lee, H.-S., *Anal. Chim. Acta* **2012,** *757*, 69-74.
9.Jokar, M., Safaralizadeh, M. H., Hadizadeh, F., Rahmani, F., Kalani, M. R., *J. Biomol. Struct. Dyn.* **2017,** *35* (2), 343-353.
10.Kavruk, M., Özalp, V. C., Öktem, H. A., *J.Anal.Methods Chem.***2013,** *2013*.
11.Barahona, F., Bardliving, C. L., Phifer, A., Bruno, J. G., Batt, C. A., *Ind.Biotechnol.***2013,** *9* (1), 42-50.
12.Bala, R., Dhingra, S., Kumar, M., Bansal, K., Mittal, S., Sharma, R. K., Wangoo, N., *Chem.Eng.J.* **017,** *311*, 111-116.
13.Bala, R., Kumar, M., Bansal, K., Sharma, R. K., Wangoo, N., *Biosens. Bioelectron.* **2016,** *85*, 445-449.

C. Supplementary figures

Figure S1

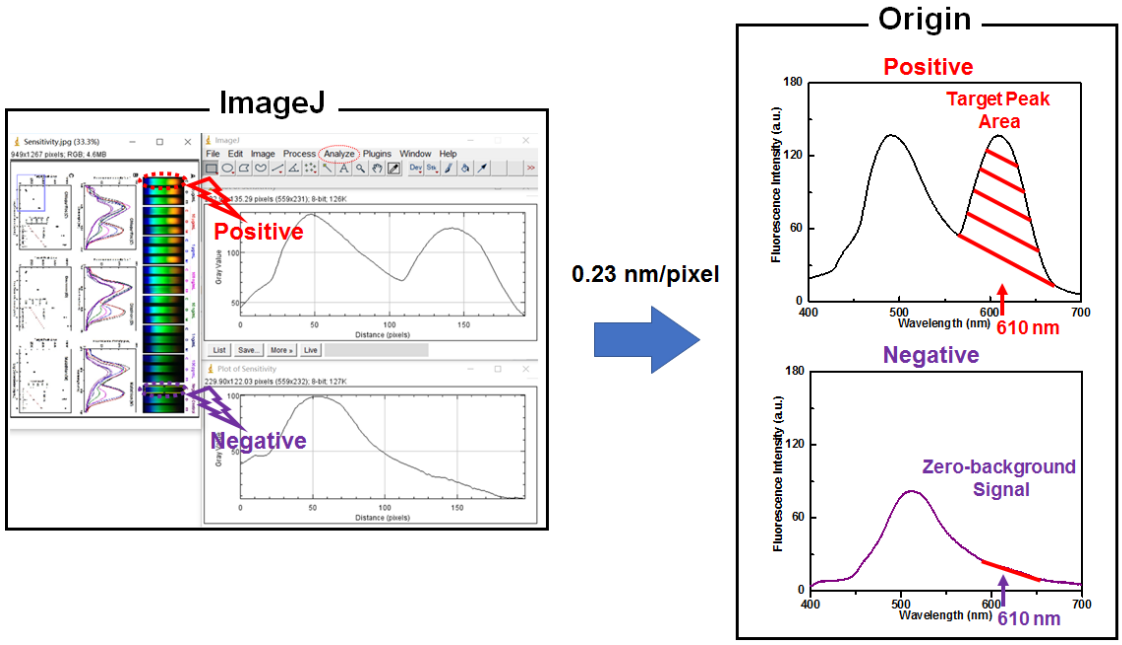

Figure S1. Data analysis strategies using two commercial software programs (ImageJ and Origin)

Figure S2

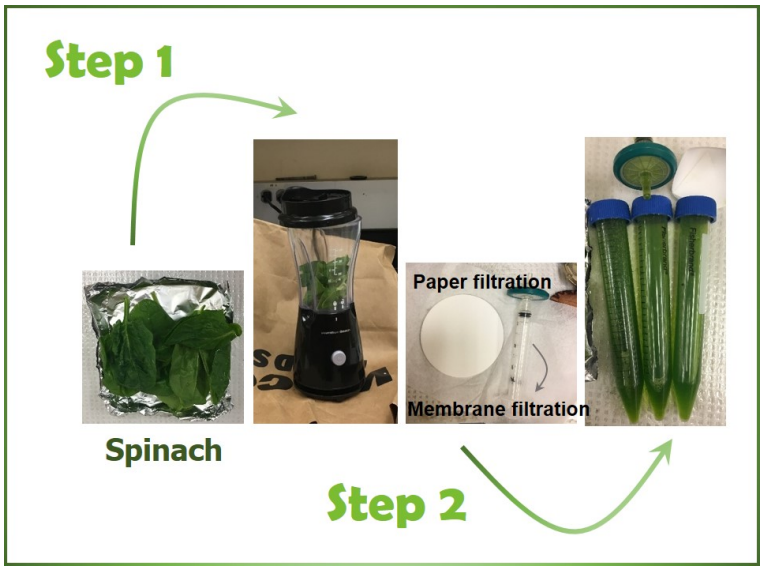

Figure S2. Preparation steps of spiked real samples

Figure S3

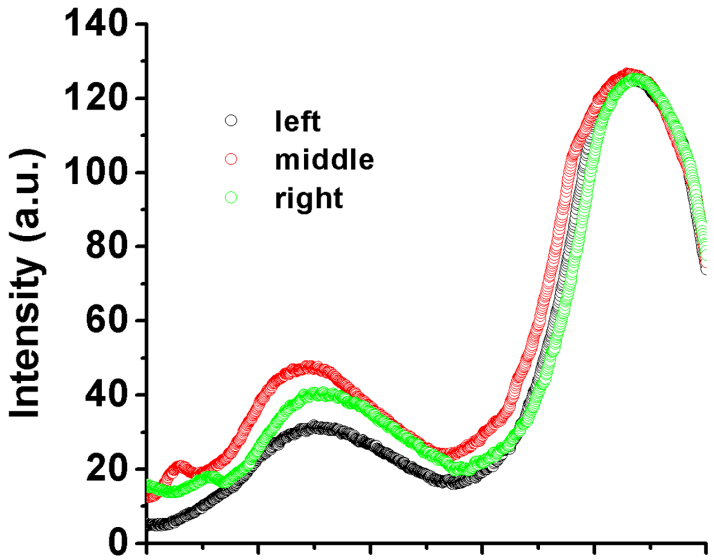

Figure S3. Light intensity distributions of three channels measured via smartphone fluorimeter

Figure S4

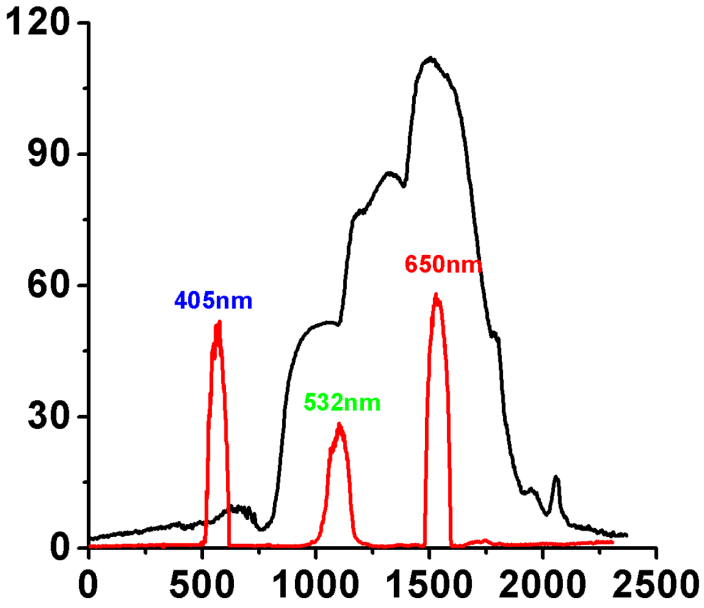

Figure S4. Light intensity distributions of three lasers (blue laser: 405 nm, green laser: 532 nm, red laser: 653.26 nm) and broadband light source (solid black line) measured via smartphone fluorimeter; corresponding wavelengths as-determined by pixel-wavelength calibration

Figure S5

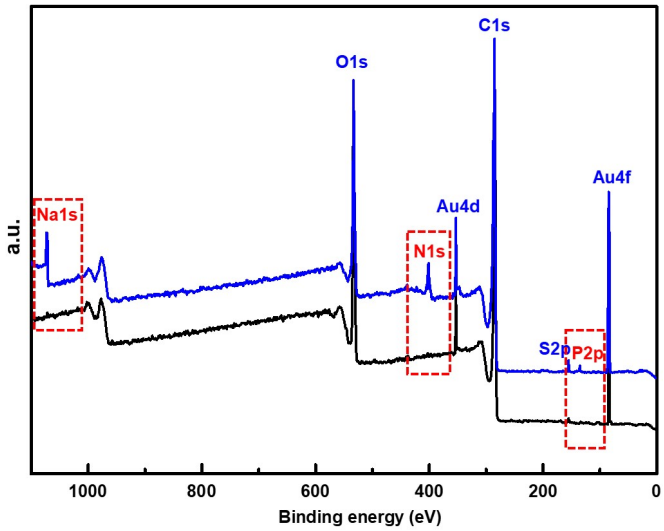

Figure S5. XPS spectrum of the synthesized AuNSs and AuNSs-aptamer probes.

Figure S6

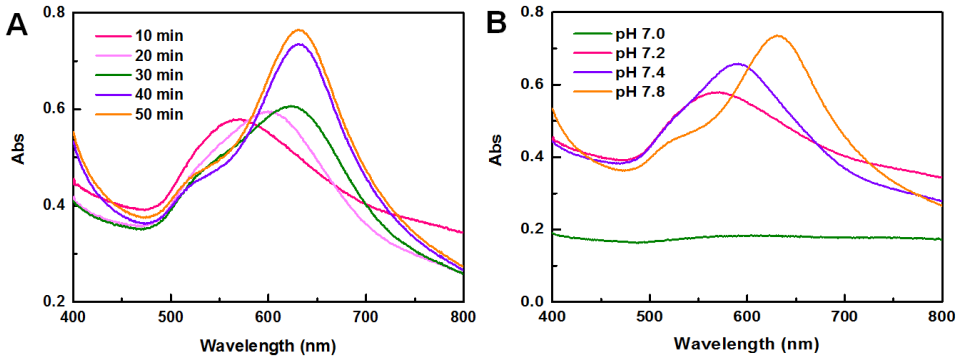

Figure S6. Impact factors of AuNSs synthesis investigated by UV-vis spectra. (A) Effect of different synthesis time:10 min, 20 min, 30 min, 40 min and 50 min; pH: 7.8. (B) Effect of various pH for AuNSs synthesis: 7.0, 7.2, 7.4, and 7.8; synthesis time: 40 min.

Figure S7

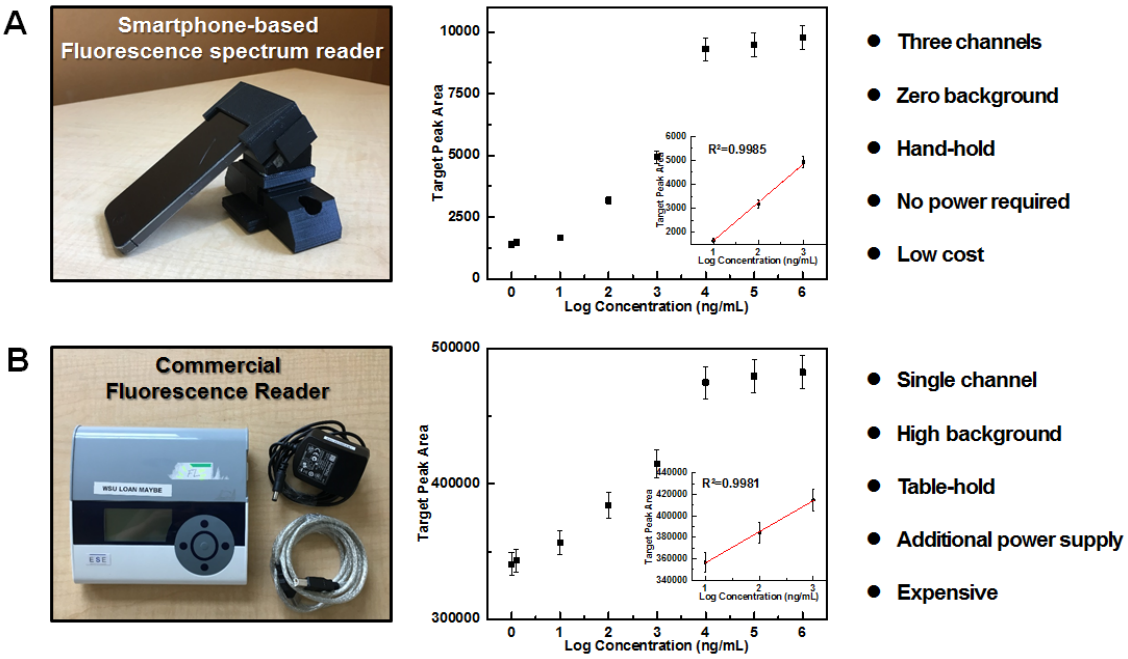

Figure S7. Comparison of proposed smartphone-based fluorescence spectrum reader (A) and commercial fluorence reader (B)

Figure S8

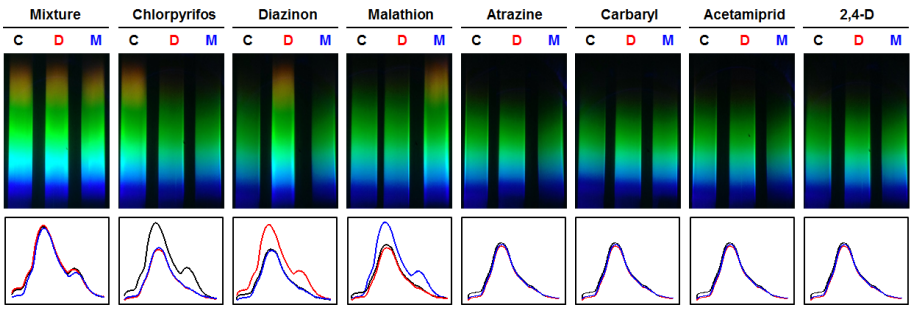

Figure S8. Specificity of the apta-LFB system investigated by smartphone spectrum reader. Typical images of different samples: a mixture of 10 ng/mL chlopyrifos (C), 10 ng/mL diazinon (D), and 10 ng/mL malathion; 10 ng/mL chlopyrifos; 10 ng/mL diazinon; 10 ng/mL malathion; 10 ng/mL atrazine; 10 ng/mL carbaryl; 10 ng/mL acetamiprid; and 10 ng/mL 2,4-D.

Figure S9

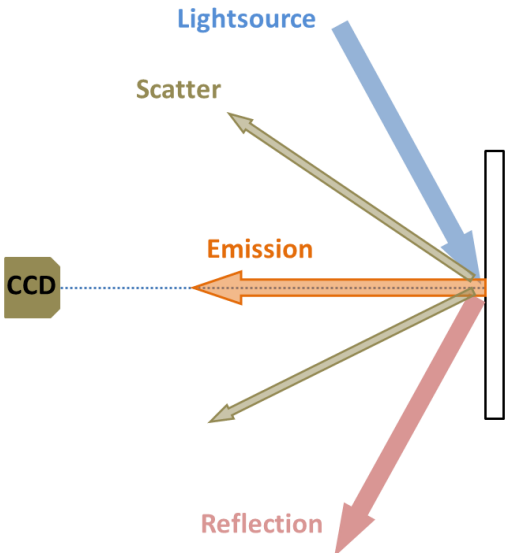

Figure S9. Reflectometer: standard detection modality for analyzing test strips with increasing SNR ratio where detector receives little scattered light from the nitrocellulose membrane

Figure S10

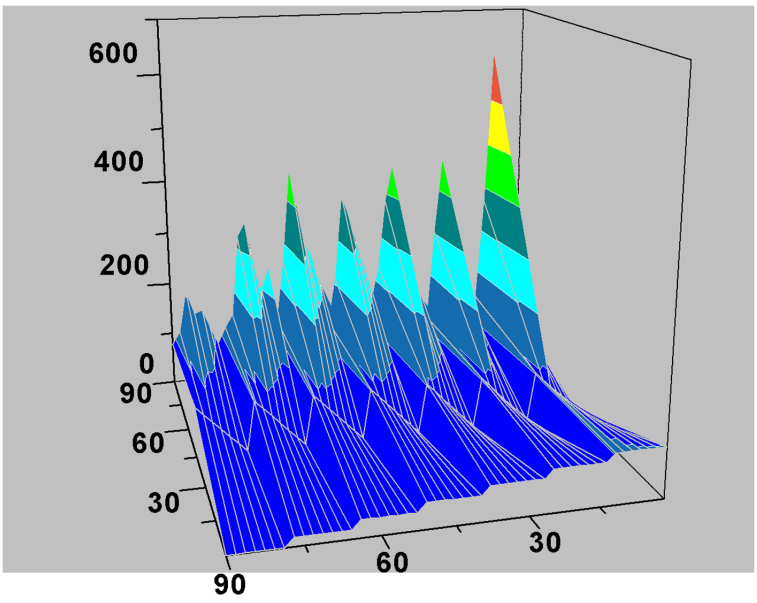

Figure S10. Nitrocellulose optimaize experiments showing dual points for improved SNR ratio; optimal configuration is lightsource 60 degrees from detection point, detector 90 degrees from surface